



Globus-M Results Toward with enhanced

V.K. Gusev, N.N. Bakharev, A.A. Berezutskii, V.V. Bulanin, A.S. Bykov,
S.E. Bender, F.V. Chernyshev, I.N. Chugunov, V.V. Dyachenko, A.D. Iblyaminova,
M.A. Irzak, A.A. Kavin, G.S. Kurskiev, S.A. Khitrov, N.A. Khromov, V.A. Kornev,
M.M. Larionov, K.M. Lobanov, A.D. Melnik, V.B. Minaev, A.B. Mineev, M.I. Mironov,
I.V. Miroshnikov, A.N. Novokhatsky, A.D. Ovsyannikov, A.A. Panasenkov, M.I. Patrov,
M.P. Petrov, Yu.V. Petrov, V.A. Rozhansky, V.V. Rozhdestvensky, A.N. Saveliev,
N.V. Sakharov, P.B. Shchegolev, O.N. Shcherbinin, I.Yu. Senichenkov,
V.Yu. Sergeev, A.E. Shevelev, A.Yu. Stepanov, S.Yu. Tolstyakov, V.I. Varfolomeev,
A.V. Voronin, E.G. Zhilin, A.Yu. Yashin, F. Wagner, E.A. Kuznetsov, V.A. Yagnov

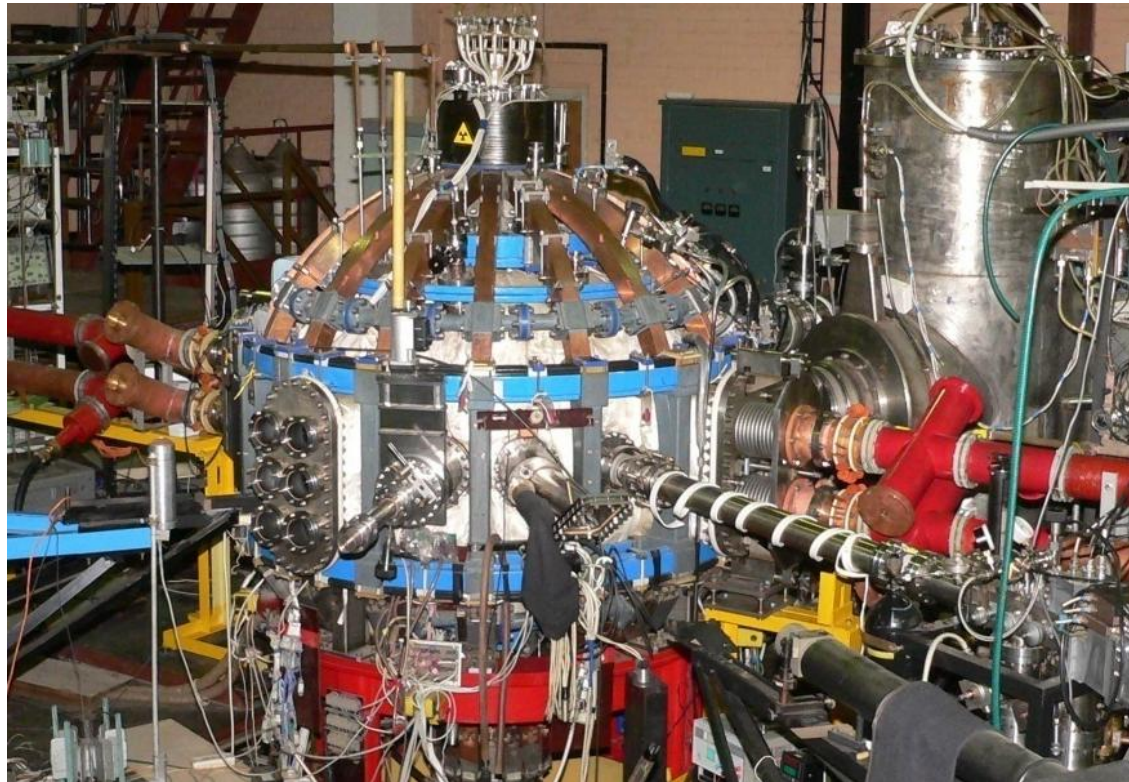
Compact Spherical Tokamak

Parameters Globus-M

- A.F. Ioffe Physico -Technical Institute, Russian Academy of Sciences, St. Petersburg, Russia
- Saint Petersburg State Polytechnical University, St. Petersburg, Russia
- D.V. Efremov Institutes of Electrophysical Apparatus, St. Petersburg, Russia
- Saint Petersburg State University, St. Petersburg, Russia
- IPT RRC “Kurchatov Institute”, Moscow, Russia
- Ioffe Fusion Technologies Ltd, St. Petersburg, Russia
- RLPAT Saint Petersburg State Polytechnical University, St. Petersburg, Russia;
Max-Planck Institute, Greifswald, Germany
- TRINITI, Troitsk, Moscow, Russia

EX 8/3

Globus-M spherical tokamak demonstrated practically all of the project objectives

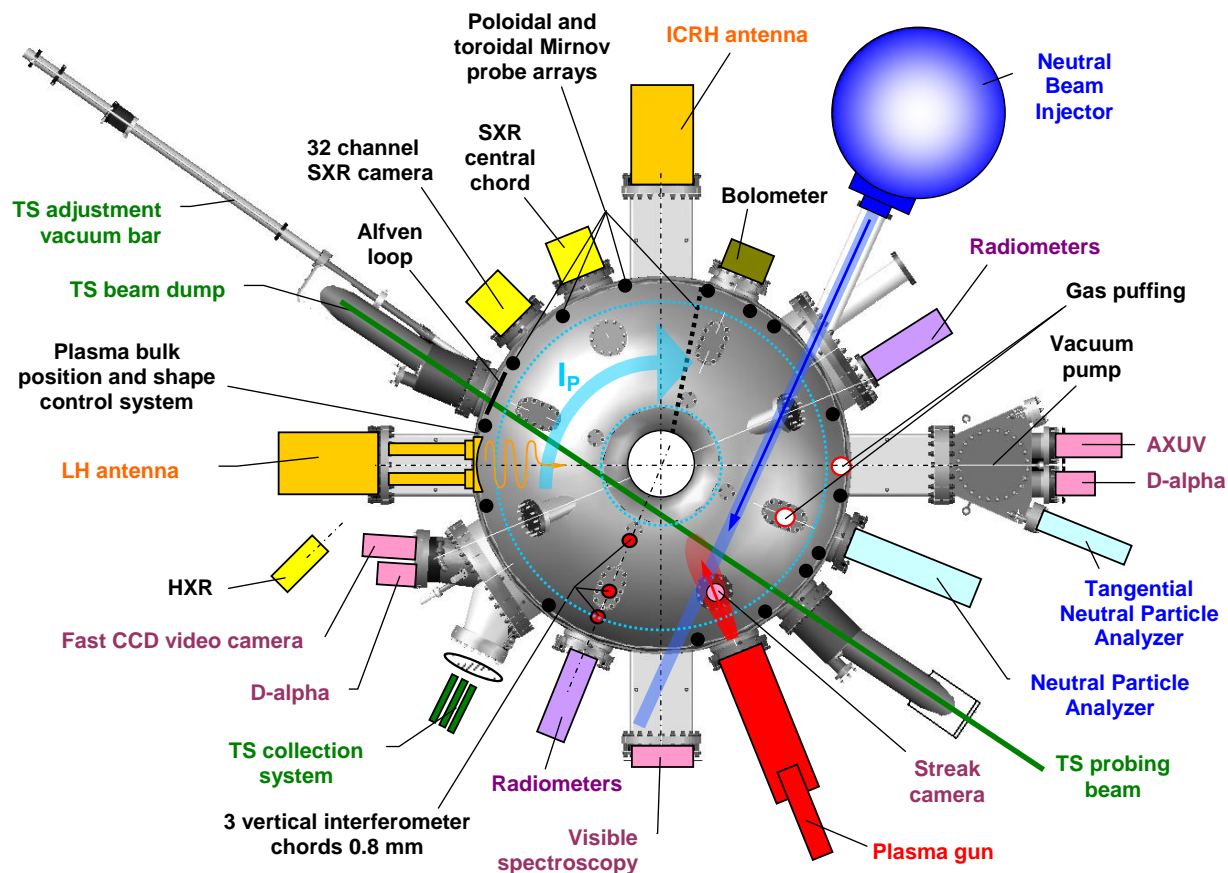


R	0.36 m
a	0.24 m
R/a	1.5
B _{tor}	0.4 T
I _{pl}	< 0.36 MA
κ	< 2.0
δ	< 0.5
β _{tor}	<15 %
β _N	<6.0 %mT/MA
T _{pulse}	<130 ms
NBI [E/P]	30 keV / 1 MW
ICRH [F/P]	10 MHz / 0.3 MW
T _e [max]	~1 keV
T _i [max]	~0.8 keV
q ₉₅ [min]	>2
B _{tor} /R	<1.5 T/m
<n> [max]	<1.2 · 10 ²⁰ m ⁻³

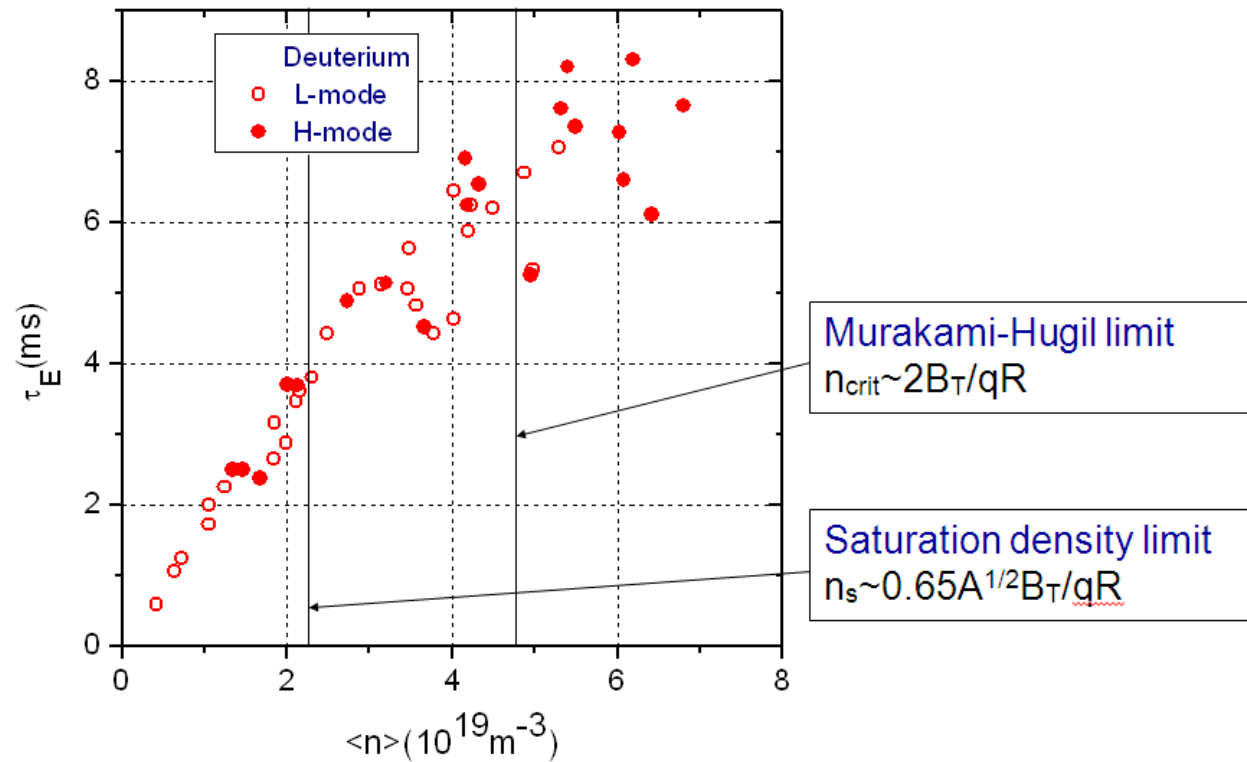
Maximal T and n values were obtained in different regimes

Globus-M:

- Close fitting wall;
- RGT tiles;
- Plasma gun;
- LH CD system



NB injection is the major instrument for plasma auxiliary heating in Globus-M



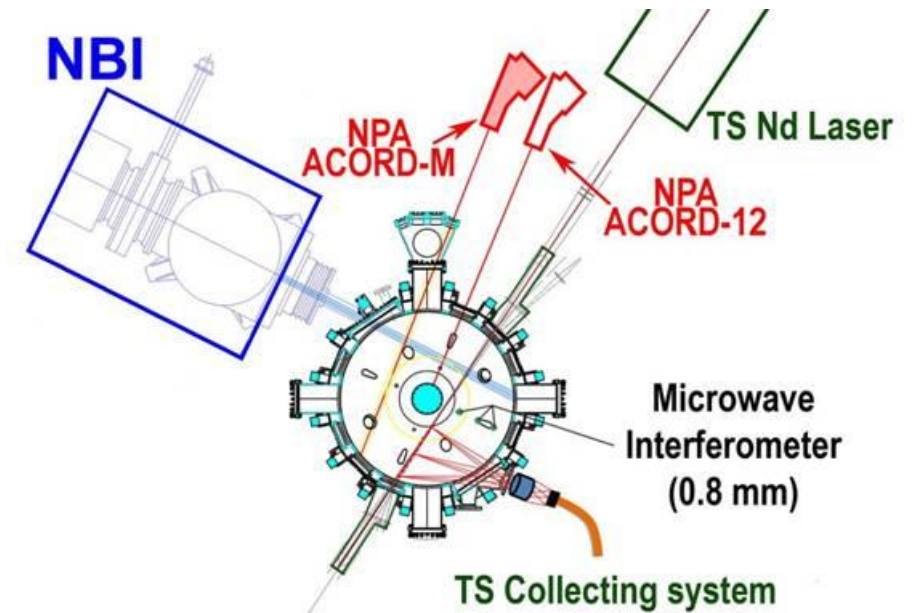
Linear lifetime dependence is characteristic for small size machines with domination of electron heat transport, e.g. Alcator-A, ISX-B, etc

During isotope effect study in Globus-M almost linear τ_E dependence on plasma density was measured in the wide density range. Both L- and H-mode data are shown.

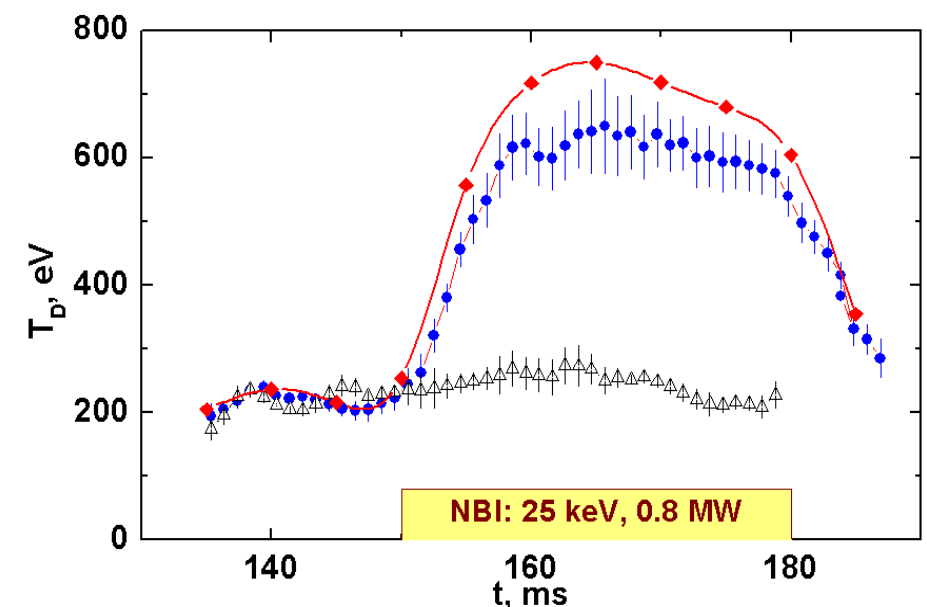
Approximate values of saturation density limit, (left) and Murakami-Hugill limit, (right) are shown.

Such energy lifetime dependence is characteristic for small size machines with domination of electron heat transport. In such a regimes ion transport virtually do not play a role.

Electron heat transport in Globus-M is strongly anomalous.



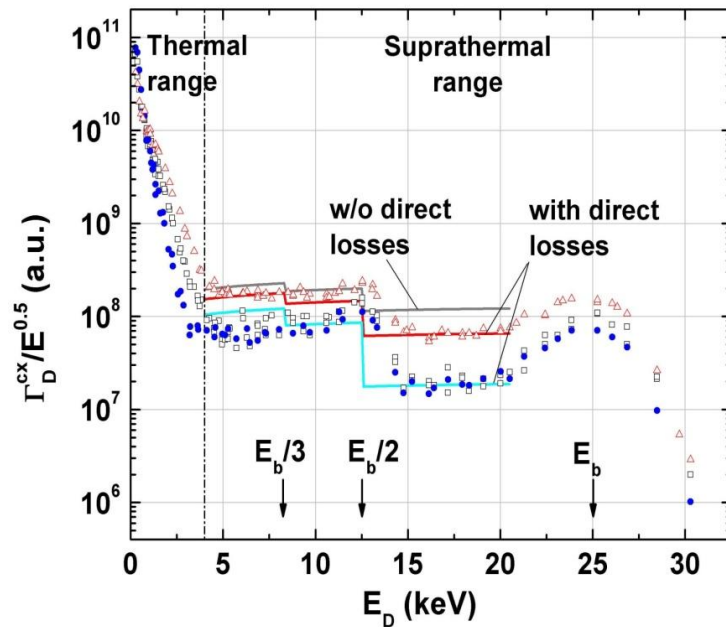
In spite of difficulties connected with a compact size of the machine NBI ion heating efficiency is reasonable, however the density range is narrow: $(2-4) \cdot 10^{19} \text{ m}^{-3}$.



Modeling demonstrates that ions are neoclassical in the wide density range.

Globus-M confinement, heating, fast particle and edge plasma physic result issues

- “Horizontal” lines approximate Fokker-Plank equation solution with slowing down losses and allow for direct losses estimate



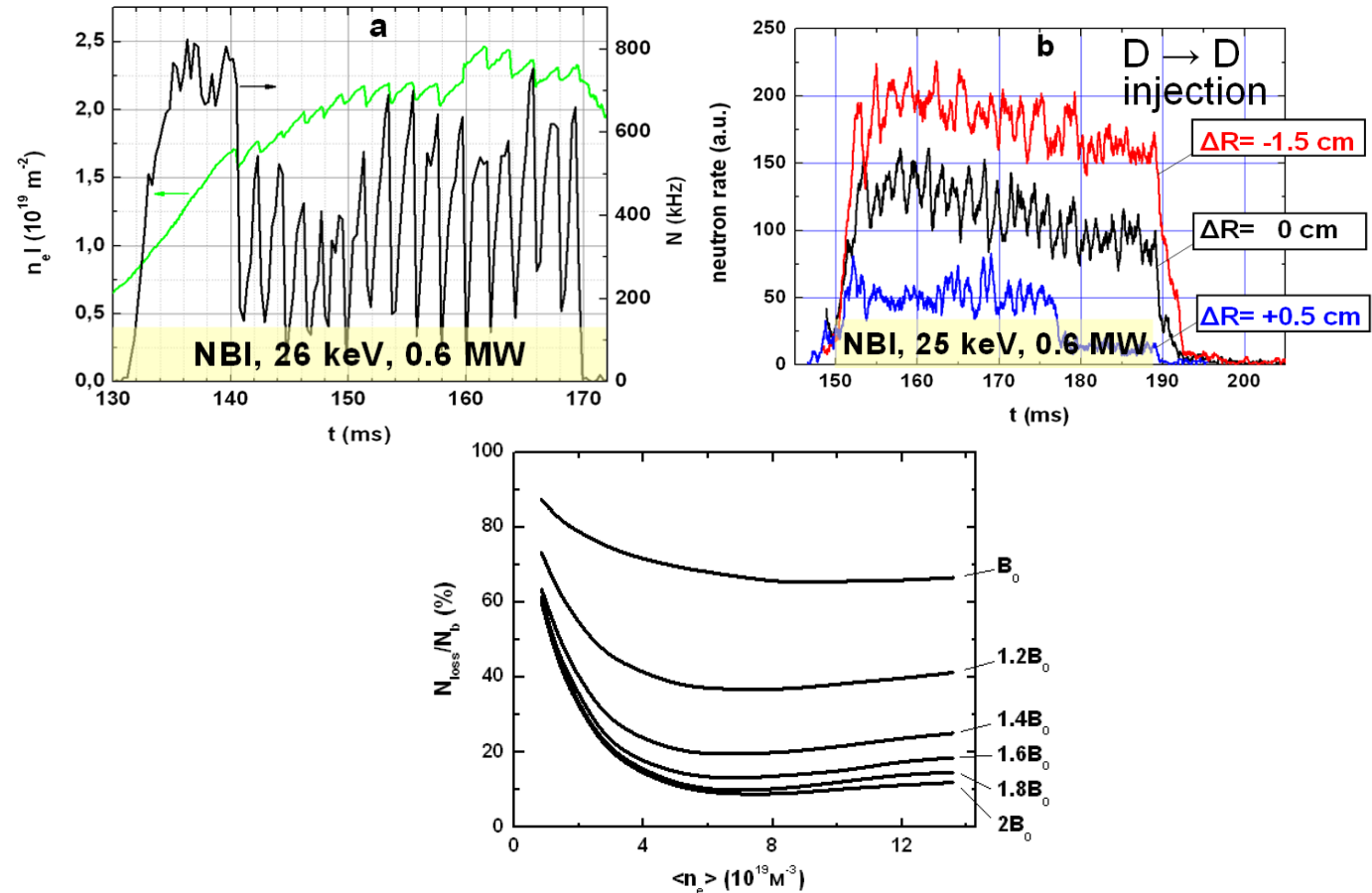
NB heating may be more efficient in Globus-M, but big losses of fast particles from bad orbits are recorded.

Three positions of plasma columns were investigated. Inward shift by 1.5 cm, usual position and outward shift by 0.5 cm.

Theoretical approximation of the spectra by Fokker-Plank equation solution with the losses during slowing down are shown. The assumption of no direct losses is shown by the grey lines parallel to the X-axis. S

Significant first orbit losses are recorded in the case of usual and shifted outward plasma column position. They reached 50% and more.

Sawteeth are responsible for additional fast particle direct losses, producing “bump on tail” distribution



Additional losses are connected with sawteeth development. The coincidence of sawteeth phase and fast particle flux of high energy is recorded. After sawteeth start the flux of fast particles drops sharply.

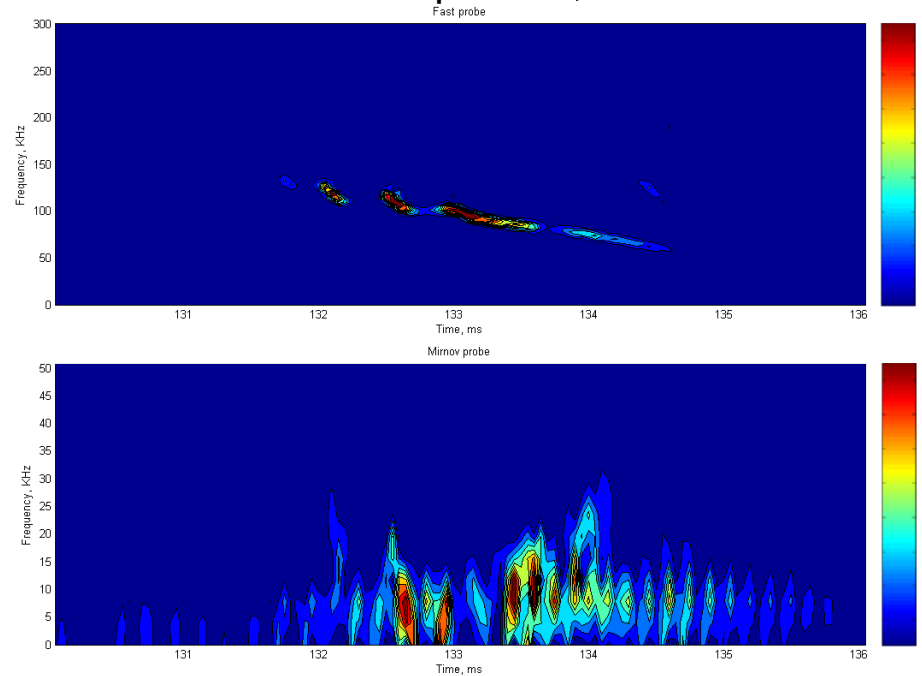
D-D neutron flux rate during D-beam injection into D-plasma it is modulated by sawteeth (sawteeth losses) and dependent on the plasma position (bad orbits losses).

The sawteeth effect could increase fast particle losses by another 20-30% (70-80% in total).

Simulations shows several time losses decrease if the magnetic field doubles from 0.4 to 0.8 T.

TAE single n=1 mode excitation is experimentally recorded in Globus-M providing no extra fast particle losses likely in Globus-M2 too

H-NBI into D-plasma, E= 27 keV



MHD fast particle instabilities do not introduce additional fast particle losses. High frequency (upper box) MHD and low frequency instabilities driven by fast particles are recorded.

Unlike the NSTX and MAST we recorded single n=1 Toroidal Alfvén Eigenmodes excitation. This favorable situation will be conserved at the highest value of magnetic field even at the beam particle energy increase up to 120 keV.

•Magnetic field 2.5 fold increase make it possible 6 fold beam energy increase without TAE spectrum enrichment:

$$V_b/V_A \approx 1 \text{ on Globus-M} \quad V_b/V_A \sim \sqrt{E_b/B} \text{ at } n_e = \text{const}$$

•Unlike TAE EPM is recorded as multimode excitation

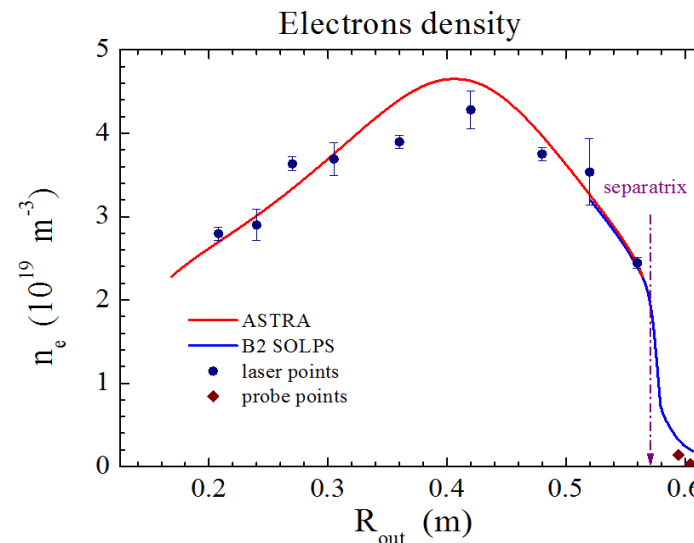
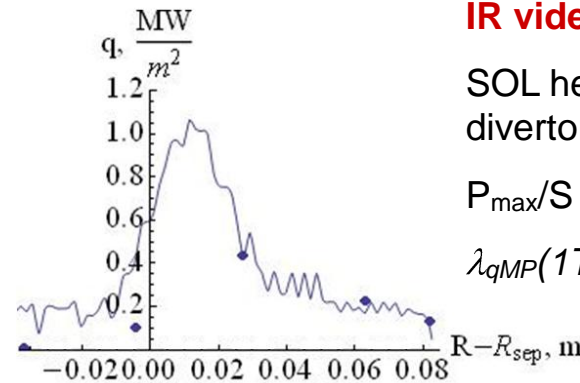
Prospects for edge plasma parameters is important issue for the upgraded machine

IR videocamera and Langmuir probes data:

SOL heat flux e-folding length, $\lambda_{qMP} \approx 3-5 \text{ mm}$ SOL divertor plates width, $\lambda_{qD} \approx 15-20 \text{ mm}$

$P_{\text{max}}/S \approx 1.1 \text{ MW/m}^2$ (OH LSN discharge)

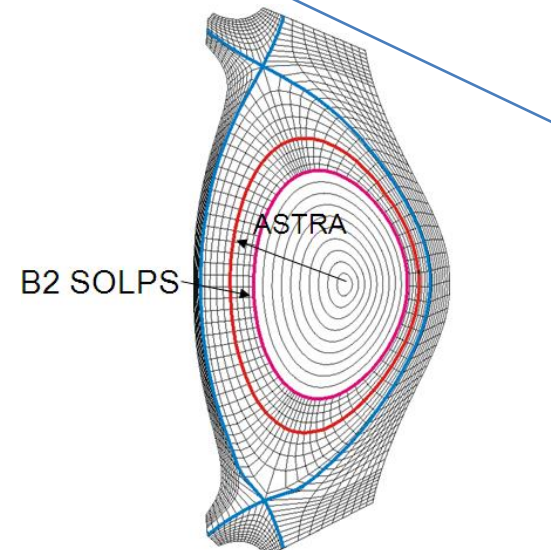
$$\lambda_{qMP}(1T) = 2ap/R \sim 2a\sqrt{T_i}/RB_{pol} \sim \lambda_{qMP}(0.4T)$$



In DN shot, the heat flux density is reduced to 0.6 MW/m².

Estimates for the upgraded machine shows that SOL width does not change significantly.

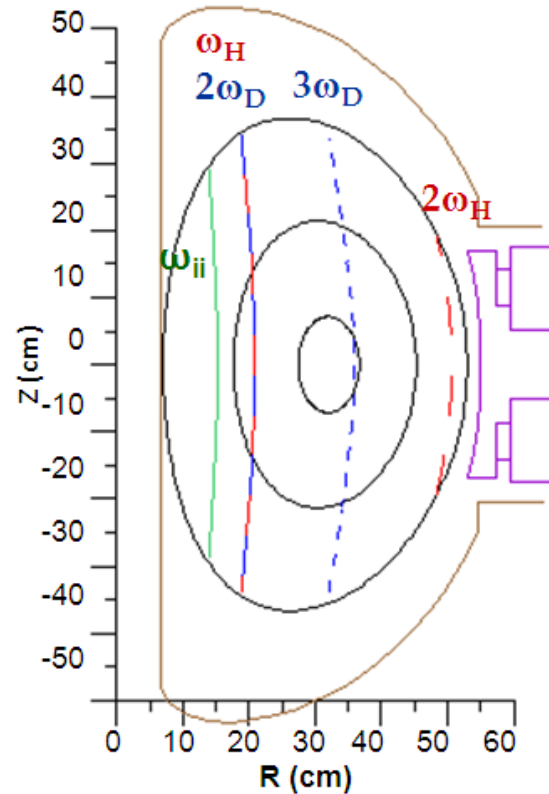
Important that the particle and heat flux are nearly equally divided between the first wall and diverter plates.



Simulation results of 1-D ASTRA transport code and 2-D B2SOLPS. Both codes were used in a serial-iterative manner to simulate the plasma periphery and the SOL in Globus-M.

ICRH prospects for 1 T in Globus-M2

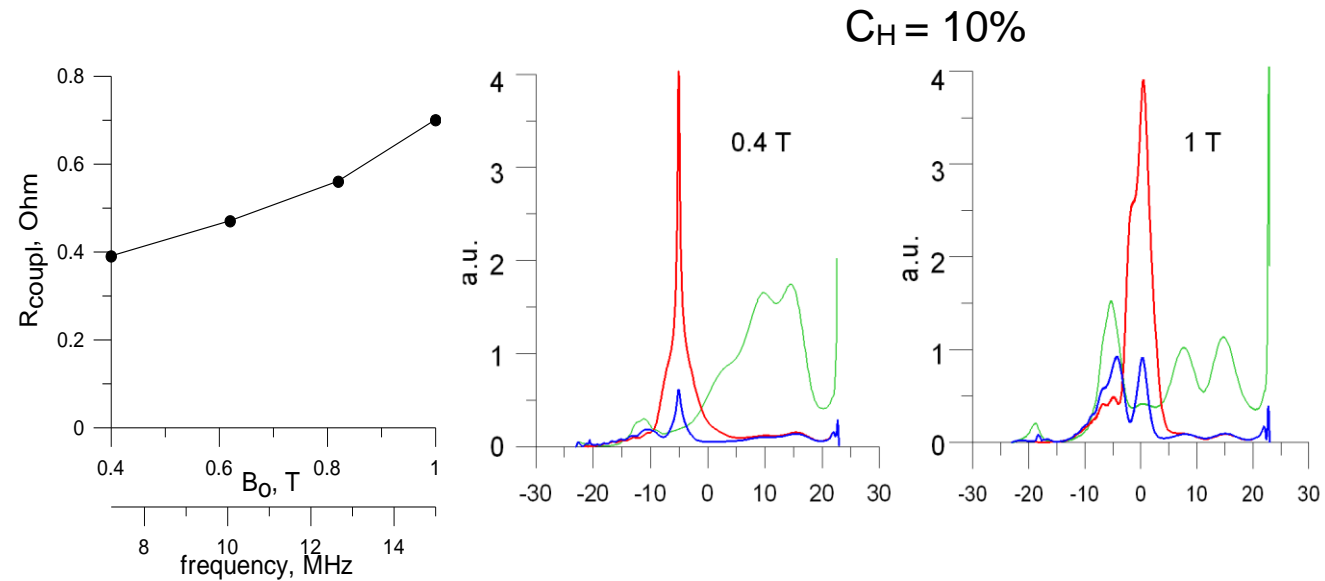
If B_T will be increase from 0.4 to 1 T what are benefits for ICRH heating by FMS waves at fundamental harmonic range?



- The same scenario with fast magnetosonic waves at the fundamental frequency range will be used at the upgraded machine.
- Whether it will be efficient at higher magnetic fields predicted for the upgraded machine?
- **Single pass resonance absorption of FMS waves increasing due to λ decrease**
- **Ion-ion hybrid resonance absorption increasing**
- **High magnetic field improves fast ion confinement and heating efficiency**

B_T	0.4T	1 T
$1f_{ci}$ for H^+	6.1 MHz	15.2 MHz

ICRH heating efficiency increases with magnetic field raise from 0.4 T to 1 T



Antenna-plasma coupling resistance raise increases RF power absorption efficiency with magnetic field

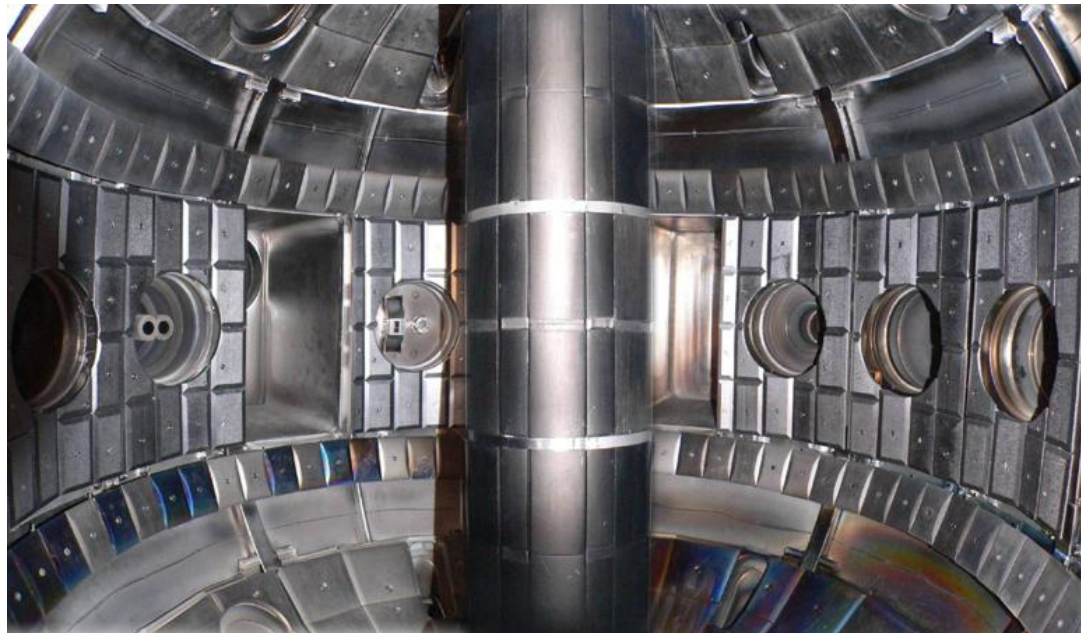
Particle	Fraction of power at 0.4 T	Fraction of power at 1.0 T
e^-	0,641	0,46
p^+	0,260	0,38
d^+	0,099	0,16

The improvements in ion cyclotron resonance heating efficiency:

The wavelength became shorter at higher magnetic field, the absorption in the resonance layers become better at the same concentration of light minority.

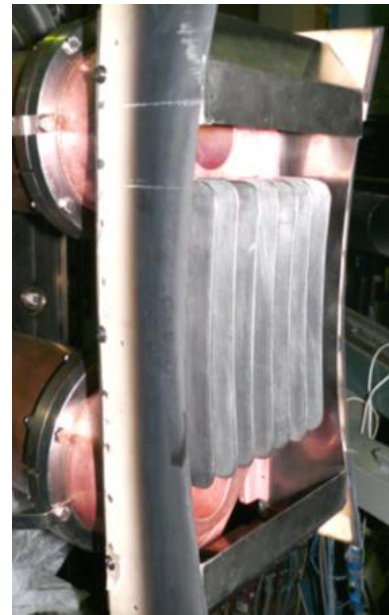
The power input into the ion component increases (see the table)

Novel experimental arrangement was used for LH CD experiment including total graphite wall protection and new antenna type



The new antennae comprises of comb-like structure, oriented toroidally was used.

Also the graphite first wall armor was returned back.



**New antennae with
“toroidal” slow down:**

$$N_{tor} \approx (6 - 7)$$

$$N_{pol} \approx 1$$



**Old antennae with
“poloidal” slow down:**

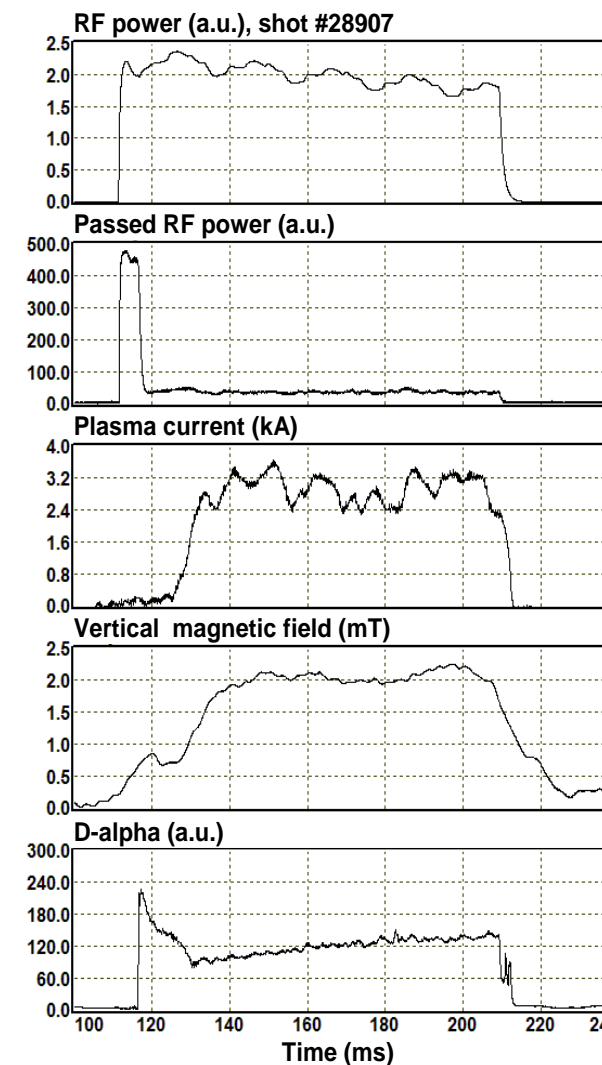
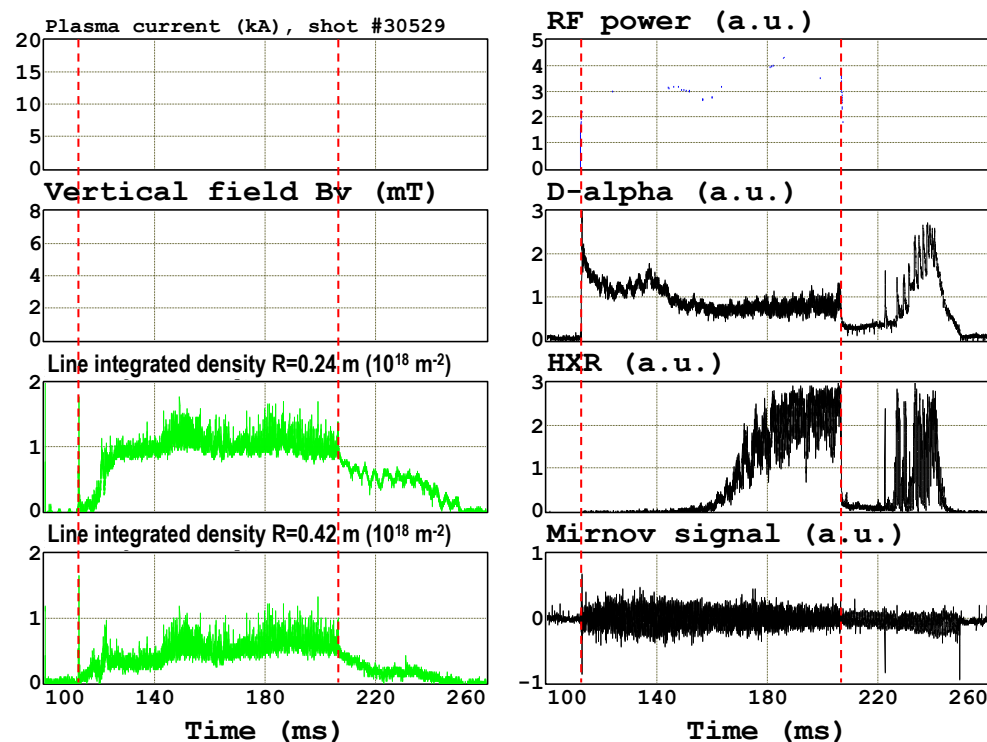
$$N_{tor} \approx (1.0 - 15)$$

$$N_{pol} \approx (7 - 8)$$

LH CD experiment in Globus-M and expectations for Globus-M2

Total driven current comprises at least by 80% of noninductively driven current by LH waves at 900 MHz and 60 kW RF power launched

During period of constant vertical field plasma current is supplied by EM waves energy



Special experiment was done with the constant poloidal magnetic field when the poloidal flux created by vertical field remains constant.

During this quasistationary stage the total plasma current is driven by RF waves.

F= 900 MHz

P=30 kW

Noninductive driven current amplitude remained at the same level.

Remarkable is a strongly improved shot reproducibility ~100%.

The contribution from poloidal (equilibrium) field coils was estimated more carefully. The results shown on the slide convinced us that at least 80% of plasma current is driven noninductively.

Contribution of the inductive PF coil flux doesn't exceed 20%

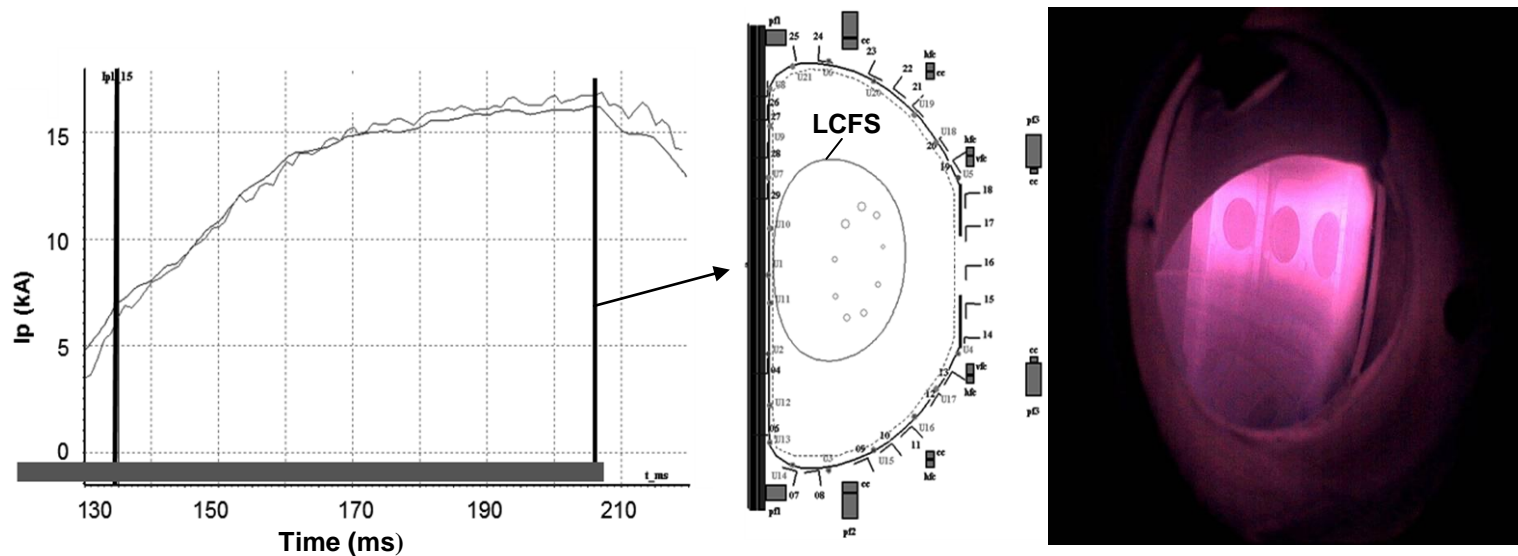
- Inductive flux of the plasma current

$$\Psi_{\text{surf}} = I_p L_{\text{ext}} = 7,1 \text{ mWb}$$

- Vertical field ramp-up flux

$$\Psi_{\text{PF}} = \Delta t_{\text{ramp-up}} U_{\text{surf}} = 1,5 \text{ mWb}$$

Noninductively driven current formats plasma column with closed magnetic surfaces



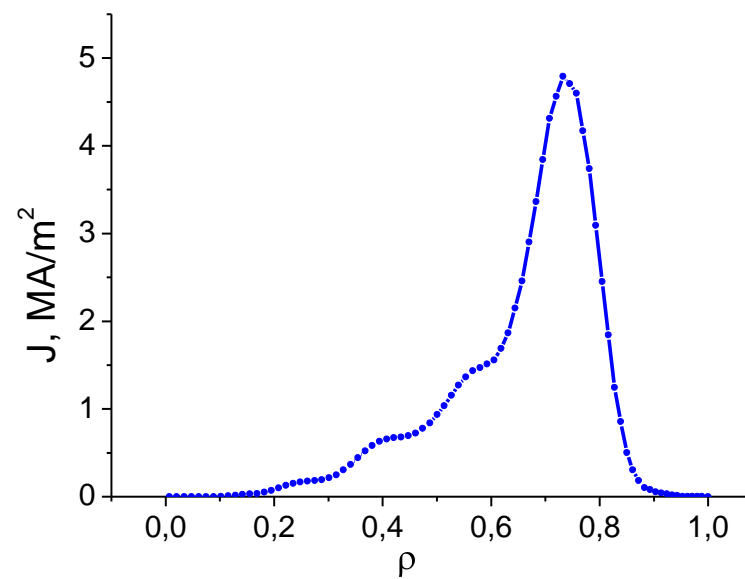
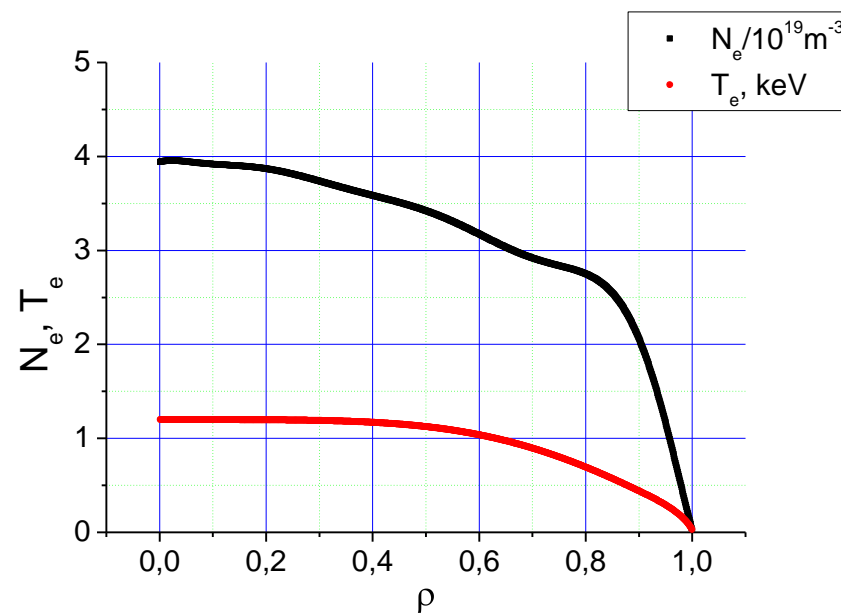
When the plasma current is less than 50 kA it is difficult to reconstruct by standard EFIT code.

A method of movable current filaments was used, allowing reconstruction of the last closed magnetic surface and external magnetic surfaces.

Plasma currents in the LH CD experiment: measured (oscillating) and reconstructed (smooth).

Video frame of the plasma shot with noninductively driven current.

Noninductive current drive simulations by LH waves demonstrated high efficiency in plasmas with increased magnetic field



F=2.45 GHz

$P_{LH} = 0.5$ MW

$B_T = 1$ T

$I_P(\text{total}) = 0.5$ MA

$I_P(\text{LHCD}) = 0.32$ MA

Profiles of plasma density and electron temperature, used in noninductive CD simulations.

Simulated current density profile for the Globus-M2 conditions. The integral value of noninductively driven plasma current is about 300 kA.

Globus-M regimes provides basis for ASTRA code modeling of Globus-M2

Instruments: ASTRA, NCLASS, NUBEAM codes

Reference case: Globus-M high density regime with $\chi_e \approx 8 \text{ m}^2/\text{s}$

Electrons heat transport

$$\tau_E^{IPB98(y,2)} \sim I_p^{0.93} \cdot B^{0.15}$$

Spherical tokamak scaling (M. Valovic et al, Nucl. Fusion, 2009, V49, p075016)

$$\tau_E^{Valovic} \sim I_p^{0.59} \cdot B^{1.4}$$

$$\chi_e^{(GI-M2)} \approx \frac{1}{2.7} \chi_e^{(GI-M)} \approx 3 \text{ m}^2/\text{s}$$

$$\chi_e^{(GI-M2)} \approx \frac{1}{6.2} \chi_e^{(GI-M)} \approx 1.3 \text{ m}^2/\text{s}$$

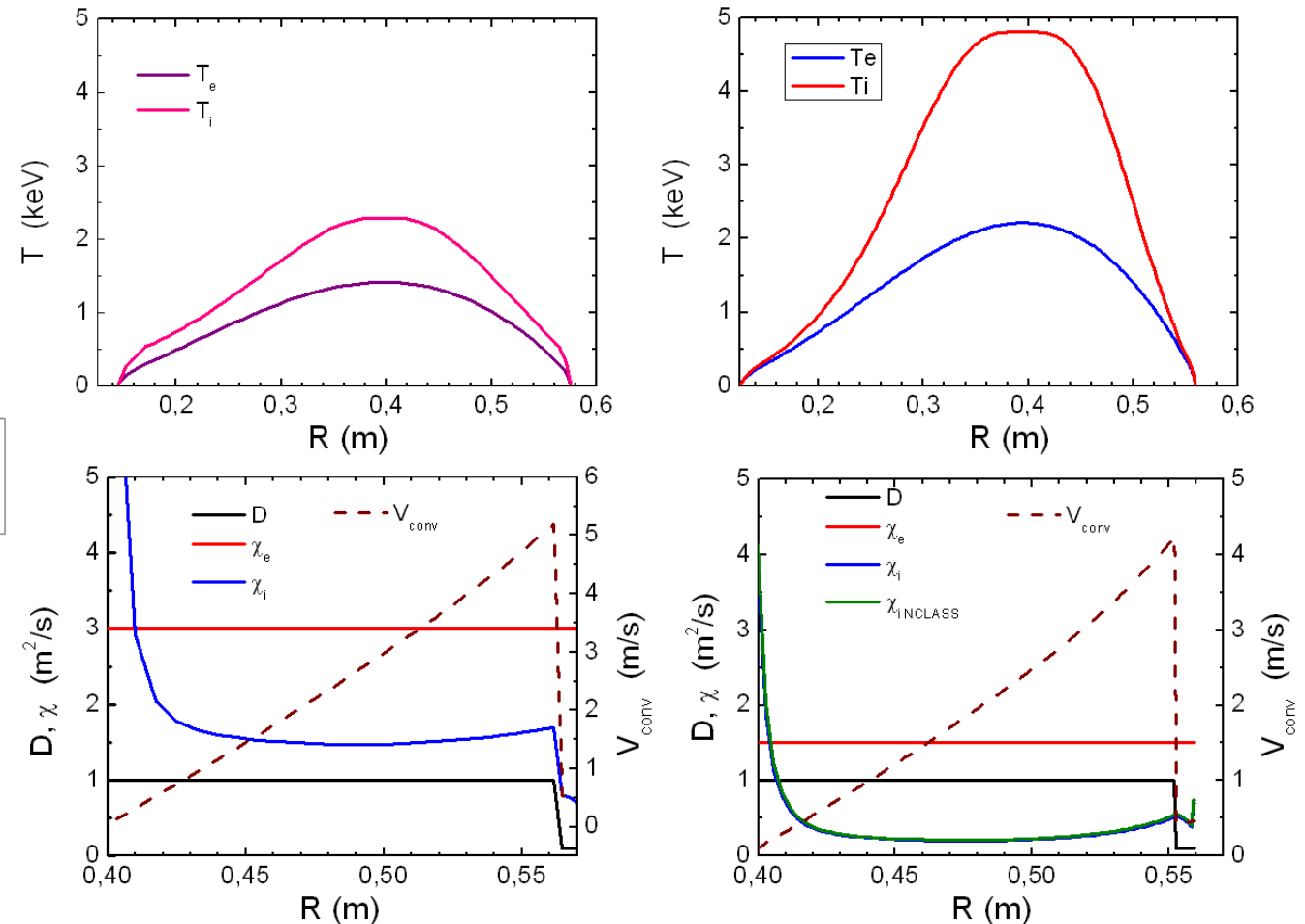
Ions heat transport

$$\chi_i = \chi_i^{NEOCL} + \chi_i^{AN}$$

$$\chi_i^{AN} \approx D$$

Particle transport – unchanged

ASTRA simulation of $E_D = 30 \text{ keV}$, $P_{NB} = 1 \text{ MW}$ NB injection into Globus-M2 discharge demonstrates high value of temperatures for density $0.7 \cdot 10^{20} \text{ m}^{-3}$



Two sets of simulations were done for neutral beam power 1 MW and energy 30 keV, which remains at the level of Globus-M experiment.

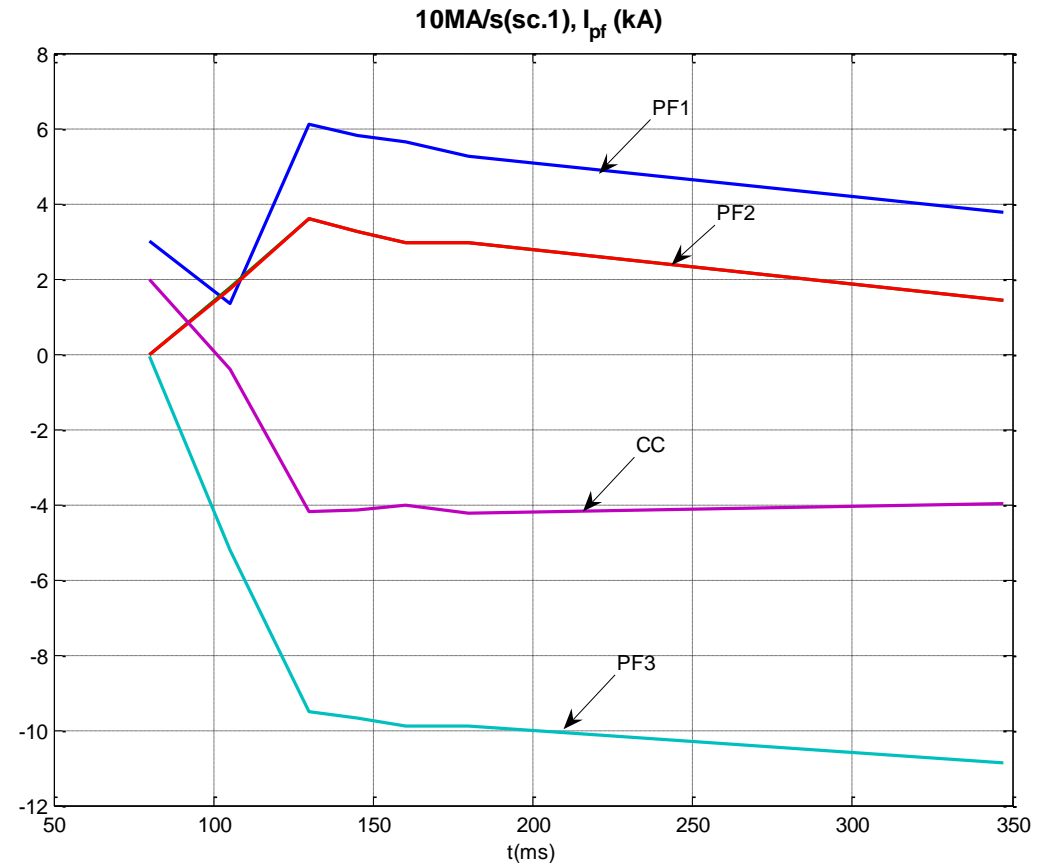
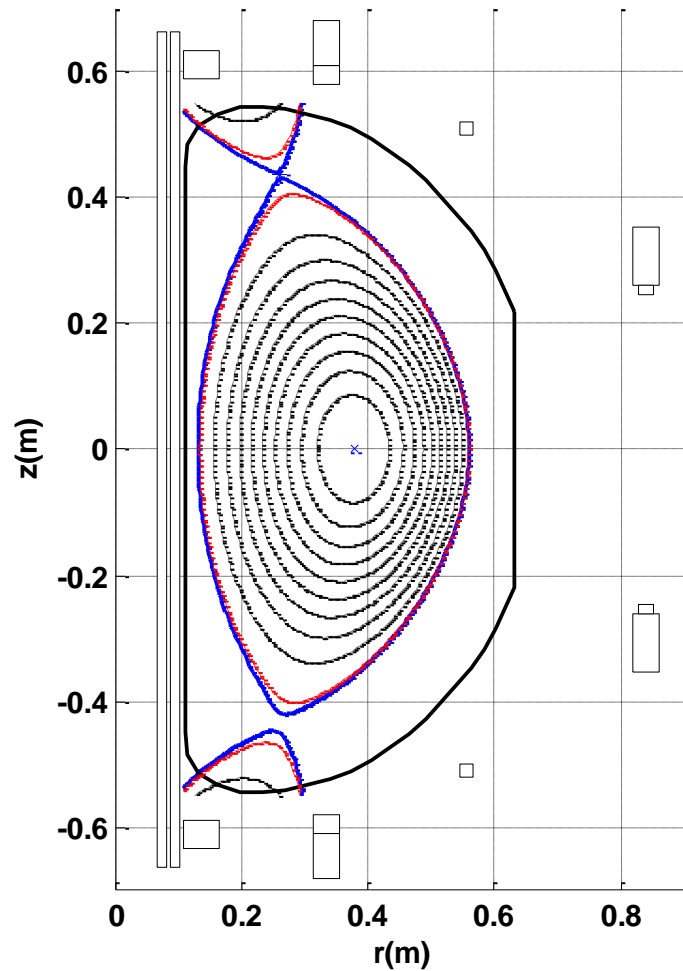
The simulated temperature profiles are shown together with transport coefficients for IPB98(y,2) (left) and ST (right) energy confinement scalings.

Plasma average density is $0.7 \cdot 10^{20} \text{ m}^{-3}$.

Super keV range of temperatures is achieved for both conservative (ITER-like) and favorable (ST-like) energy confinement scalings.

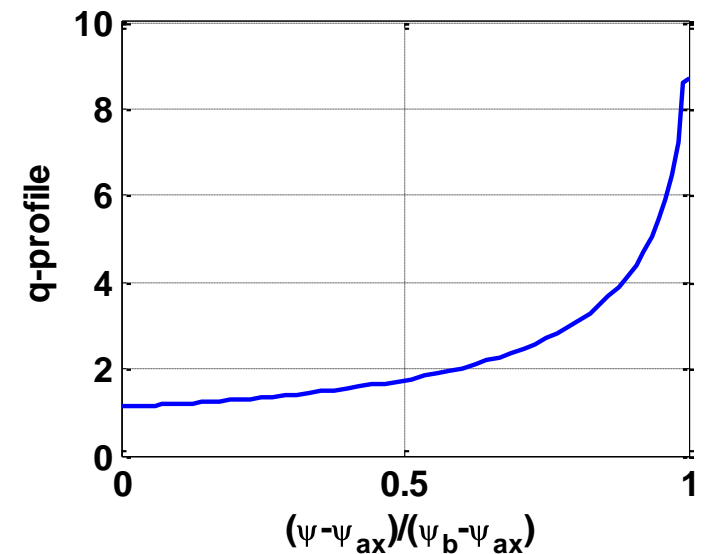
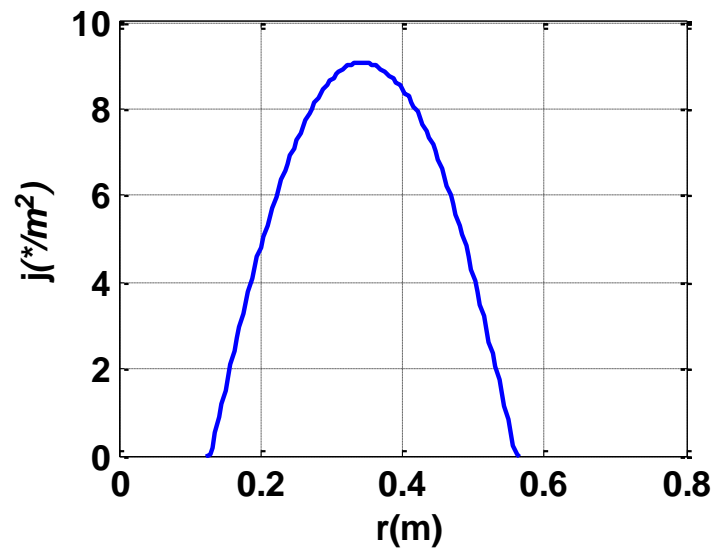
Globus-M2 parameter modeling

TRANSMARK code was used for detailed PF coil scenarios simulation



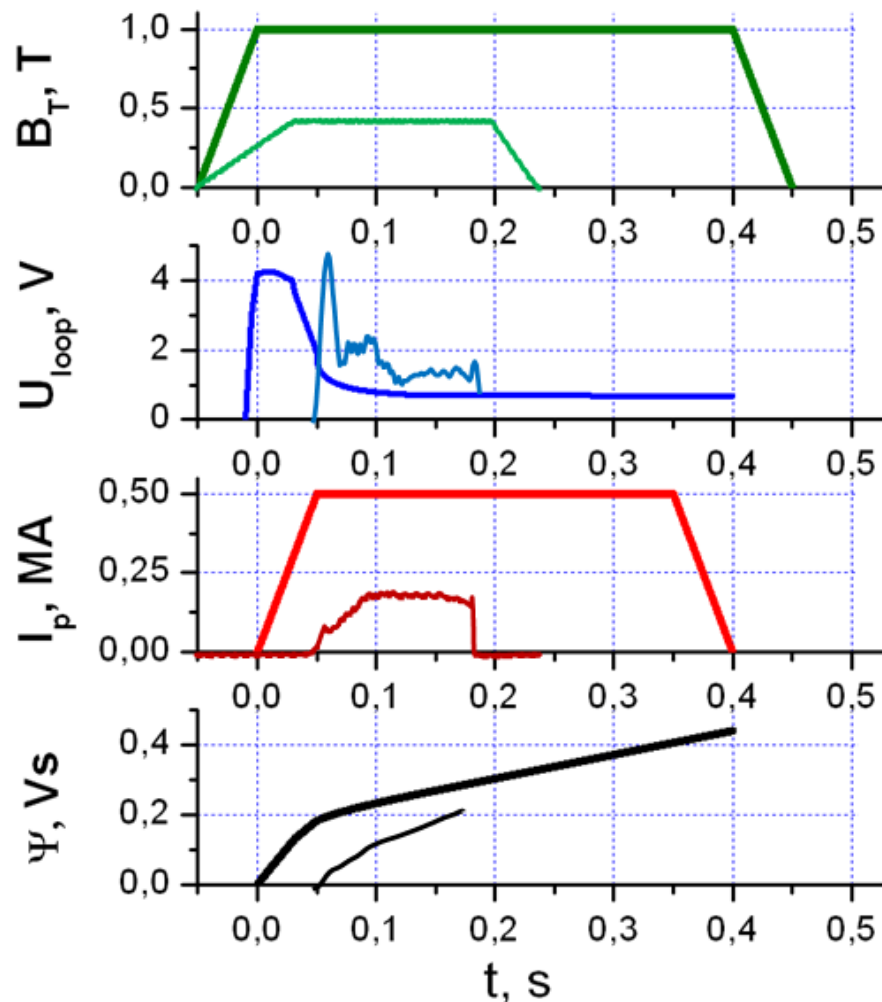
Engineering parameters and operating scenario for GLOBUS-M2 electromagnetic system were simulated with ITER scaling and TRANSMARK code.

Equilibrium double-X-point configuration with 0.5 MA current and main poloidal coils currents are shown together with current density and safety factor profiles.



Globus-M2 engineering parameter range is much wider than the Globus-M

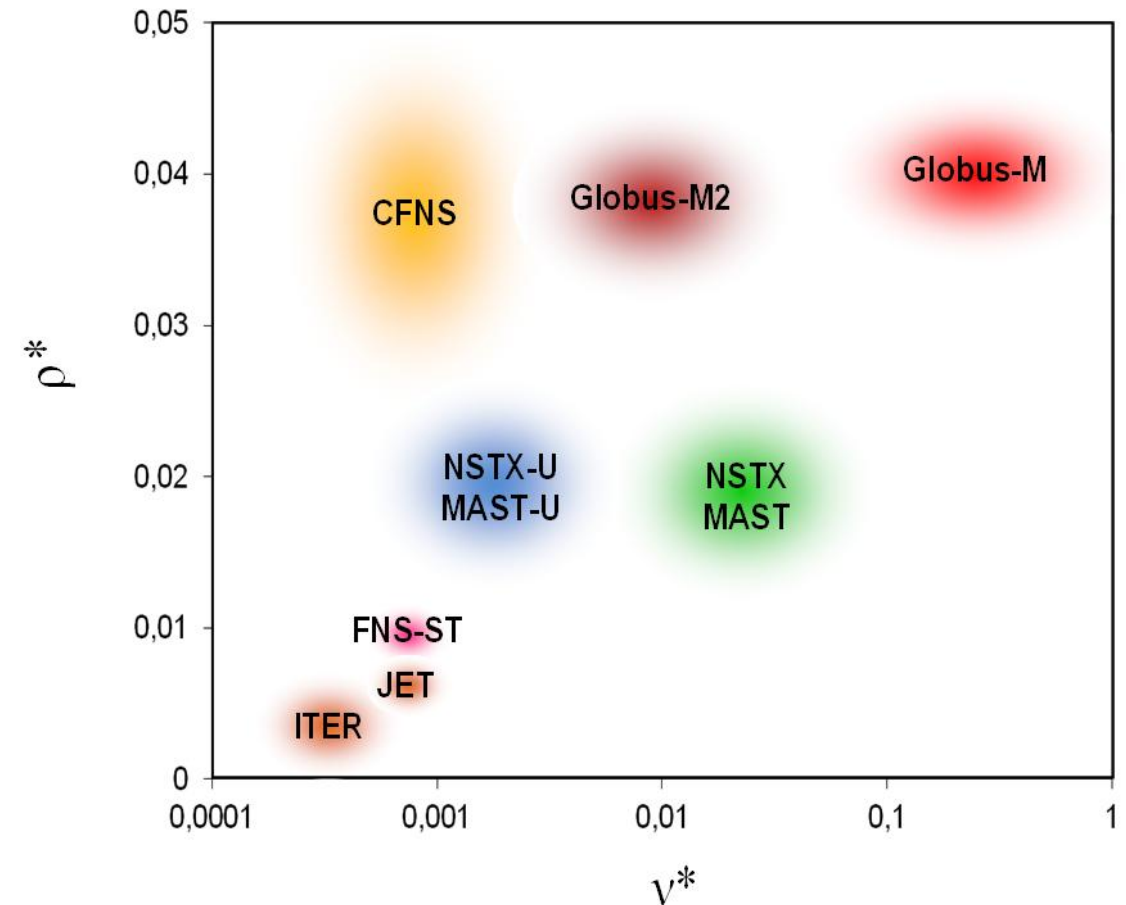
Globus-M2 “B-max” regime providing:
 $B_T(R=0.36) = 1\text{ T}$ for $\Delta t = 0.4\text{ s}$,
 $I_p = 0.5\text{ MA}$ for 0.3 sec – solid line and
 Standard Globus-M regime – thin line



Two typical regimes will be available:
 “B-max” regime providing operation at maximal toroidal field and plasma current of 0.5 MA

and
 “t-max” regime for noninductive current drive experiments providing toroidal field of 0.7 T for 0.8 sec duration.

Globus-M2 nondimensional parameters permit low collisionality regimes



Globus-M2 will operate in the low collisionality regime, which may be useful for ST confinement physics study as well as for modeling of regimes of compact fusion neutron source.

Comparison of dimensionless parameter ranges for some fusion devices is shown on the slide; (ν^* is ion core collisionality).

Conclusions

Experimental results obtained on Globus-M and modeling performed on their basis convinced us that a substantial improvement in parameters can be expected for Globus-M2 with high confidence.

For Globus-M2, the size of the plasma remains unchanged, which allows for retaining the vacuum vessel and most parts of the diagnostic and heating systems. The simulation results predict that at a plasma density up to $\sim 10^{20} \text{ m}^{-3}$ the plasmas in the tokamak Globus-M2 are heated to temperatures in the keV range with the collisionality being low. The plasma stored energy will surpass the one attained in Globus-M by a factor of 3-5.

The dimensionless parameter range for Globus-M2 allows establishing basically the conditions characteristic for a compact fusion neutron source experimental support.

Acknowledgements: The authors wish to thank dr. V.G. Merezkin from IPT Kurchatov Institute for the help in ripple losses of fast particle estimate. The work is financially supported by RAS, Minobrnauki RF, RFBR grants.

REFERENCES

- GUSEV, V.K., et al, Nucl. Fusion, 2001, **41**, No 7, 919.
GUSEV, V.K., et al, Plasma Physics and Controlled Fusion, 2003, **45**, issue 12.1, A59.
GUSEV, V.K., et al, Nucl. Fusion, 2006, **46**, No 8, S584-S591.
SHCHERBININ, O.N., et al, Nucl. Fusion, 2006, **46**, No 8, S592-S597.
GUSEV, V.K., et al, Nucl. Fusion, 2009, **49**, No 10, 104021.
GUSEV, V.K., et al, Nucl. Fusion, 2009, **49**, No 9, 095022.
GUSEV, V.K., et al, Nucl. Fusion, 2011, **51**, 103019.
GUSEV, V.K., et al, Proc. 17th IAEA Fusion Energy Conf. 1998, v.3, pp. 1139-1142.
SAKHAROV, N.V. et al, Proc. of 39th EPS Conf. on Plasma Physics, 2012, P2.004.
PARKER, R.R., et al, Nucl. Fusion, 1985, **25**, 1127.
CORDEY, J.G., et al, Nucl. Fusion, 1975, **15**, No. 3, 441.
CHERNYSHEV, F.V., et al, Plasma Phys. Reports, 2011, **37**(8), p. 553.
PETROV, Yu.V., et al, Plasma Phys. Reports, 2011, **37**(12), p. 1001.
PETROV, Yu.V., et al, Proc. of 38th EPS Conference on Plasma Physics, 2011, P-4.090.
SERGEEV, V.Yu., et al, Proc. of 39th EPS Conf. on Plasma Physics, 2012, P5.054.
GOLDSTON, R.J., et al. Nucl. Fusion, 2012, **52**, 013009.
SENICHENKOV, I.Yu., et al, Proc. of 39th EPS Conf. on Plasma Physics, 2012, P2.042.
BULANIN, V.V., et al, Technical Physics Letters 2011, **37**, p. 340.
IRZAK, M.A., et al, Plasma Phys. Reports, 1999, **25**(8), p. 601.
DYACHENKO, V.V., et al, Proc. of the 38th Conf. on Plasma Physics, 2011, P4.098.
DYACHENKO, V.V., et al, Plasma Phys. Reports, 2012, to be published.
SAVELIEV A.N., et al, Proc. of 38th EPS Conference on Plasma Physics, 2011, P4.103.
VALOVIC, M., et al, Nucl. Fusion, 2009, **49**, 075016.
MINAEV, V.B., et al, This Conference, ICC/P1-01